ELSEVIER

Biomaterials 23 (2002) 3843–3851

Biomaterials

www.elsevier.com/locate/biomaterials

Manufacture of poly(2-hydroxyethyl methacrylate-co-methyl methacrylate) hydrogel tubes for use as nerve guidance channels

Paul D. Dalton[a,c], Lauren Flynn[c], Molly S. Shoichet[a,b,c,*]

[a] *Department of Chemical Engineering and Applied Chemistry, University of Toronto, 200 College Street, Toronto, Ont., Canada, M5S 3E5*
[b] *Department of Chemistry, University of Toronto, 80 St. George Street, Toronto, Ont., Canada, M5S 1A1*
[c] *Institute of Biomaterials and Biomedical Engineering, University of Toronto, 4 Taddle Creek Road, Toronto, Ont., Canada, M5S 3G9*

Received 9 April 2001; accepted 10 March 2002

Abstract

Hydrogel tubes of poly(2-hydroxyethyl methacrylate-co-methyl methacrylate) (p(HEMA-co-MMA)) made by liquid–liquid centrifugal casting are being investigated as potential nerve guidance channels in the central nervous system. An important criterion for the nerve guidance channel is that its mechanical properties are similar to those of the spinal cord, where it will be implanted. The formulated p(HEMA-co-MMA) tubes are soft and flexible, consisting of a gel-like outer layer, and an interconnected macroporous, inner layer. The relative thickness of the gel phase to macroporous phase is controlled by the formulation chemistry, and specifically by the ratio of co-monomers, HEMA and MMA. By varying the surface chemistry of the mold within which the tubes are synthesized, tubes were prepared with either a "cracked" or a smooth outer morphology. Tubes with the cracked outer morphology had periodic channels that traversed the wall of the tube, which resulted in a lower modulus than smooth outer morphology tubes, yet likely greater diffusive permeability. For tubes (and not rods) to be formed, phase separation must precede gelation as is detailed in a formulation phase diagram for HEMA, MMA and water. The tensile elastic modulus of p(HEMA-co-MMA) tubes reflected the formulation chemistry, with greater moduli (up to 400 kPa) recorded for tubes having 10 wt% MMA. The p(HEMA-co-MMA) tubes therefore had similar mechanical properties to those of the spinal cord, which has a reported elastic modulus range between 200 and 600 kPa.

Keywords: 2-Hydroxyethyl methacrylate; Phase separation; Tubes; Liquid–liquid centrifugal casting; Nerve regeneration; pHEMA; HEMA

1. Introduction

Hydrogels are used in numerous soft tissue biomedical devices [1–3], yet their use as nerve guidance channels has been limited, perhaps because there are few methods available to form tubular shapes from crosslinked polymers [4,5]. We are pursuing an entubulation strategy for nerve regeneration where either end of a severed spinal cord is inserted into either end of a mechanically similar hydrogel guidance channel, which then provides a pathway for regeneration after injury. Such an entubulation strategy is popular in peripheral nerve regeneration studies, where regeneration in autologous nerve grafts and tubes have comparable outcomes over short gaps [6,7]. By using tubes with an elastic modulus similar to the spinal cord, we hope to generate an environment that is favorable for axonal regeneration in vivo. Further in vivo experiments can then determine the efficacy of molecular, cellular or tissue engineering therapies in regeneration.

The entire spinal cord, including the pia, has an elastic modulus ranging between 230 and 600 kPa, depending on the species, the measuring system used, and the time after death [8–11]. A mechanical measurement of the spinal cord is difficult as even short times following death significantly increase the modulus. Chang et al. [11] conducted a comprehensive study on the mechanical properties of the spinal cord in the feline model and approximated the elastic modulus of the cat spinal cord to be 230 kPa.

Synthetic tubular materials that have been previously implanted in the nervous system include poly(acrylonitrile-co-vinyl chloride) [12–15], polycarbonate [16], poly(ethylene-co-vinyl acetate) [17] and collagen [18,19].

*Corresponding author. Department of Chemical Engineering and Applied Chemistry, University of Toronto, 200 College Street, Toronto, Ont., Canada, M5S 3E5. Tel.: +1-416-978-1460; fax: +1-416-978-8605.

E-mail address: molly@ecf.utoronto.ca (M.S. Shoichet).

0142-9612/02/$ - see front matter
PII: S0142-9612(02)00120-5

Despite a wealth of knowledge on compliance mismatch resulting in failure of other implants, such as vascular grafts and bone [20–22], previously used nerve guidance channels, with the exception of collagen, are considerably more rigid than soft spinal cord tissue. Such a mechanical mismatch may compromise the efficacy of any regenerative therapy within the guidance channel. Hydrogels may be more promising candidates for use as nerve guidance channels in the spinal cord as they have similar mechanical properties [23] and proven biocompatibility in neural tissue applications [23–25].

We recently reported a new process, termed liquid–liquid centrifugal casting that creates concentric, water swollen poly(2-hydroxyethyl methacrylate) (pHEMA) tubes [26]. An initiated homogeneous monomer mixture is injected into a cylindrical mold, displacing all of the air inside, and then the cylinder is spun around its long axis (Fig. 1a). Liquid–liquid phase separation occurs when the propagating polymer radical becomes insoluble in the solvent (water). Under centrifugal forces, the denser, phase-separated monomer/polymer phase sediments at the periphery (Fig. 1b). Gelation of the phase-separated particles results in a hydrated tubular structure and water in the center of the mold. The chemistry of phase-separated pHEMA has been previously described in detail as a static process for manufacturing cell-invasive scaffolds [27–31].

Homopolymeric pHEMA tubes made using liquid–liquid centrifugal casting have highly porous walls and were considered too soft for implantation into the spinal cord [32] or the peripheral nervous system [33].

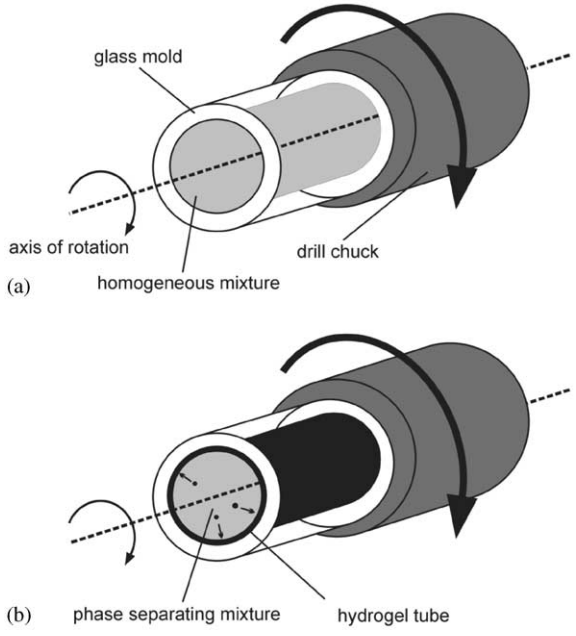

Fig. 1. Liquid–liquid phase separation is induced in a tubular mold during rotation: (a) the experimental setup and (b) a tube is formed within the glass mold.

Incorporating a hydrophobic monomer, such as methyl methacrylate (MMA), into the monomer solution accelerates phase separation and results in considerably different wall morphologies than observed for homopolymeric tubes. By varying the concentration of MMA in the formulation, both the wall morphology and the tube modulus were affected, as is described in detail herein. The focus of this paper is on the synthesis of p(HEMA-co-MMA) tubes having elastic moduli approaching a target modulus of 230 kPa, which is similar to that of the spinal cord.

2. Materials and methods

2.1. Materials

All chemicals were purchased from Aldrich Chemical Co. (Milwaukee, WI) and were used as received. Water was distilled and deionized using Millipore Milli-RO 10 Plus at 18 MΩ resistance. Aqueous solutions (10 wt%) of ammonium persulfate (APS) and sodium metabisulfite (SMBS) were used together as initiators and were made prior to every use.

2.2. Polymerization

The monomer mixture is comprised of monomers (HEMA, MMA), crosslinking agent (ethylene dimethacrylate, EDMA), and solvent (water). The formulations used are detailed in Table 1 with 25 and 30 wt% monomer mixtures having MMA concentrations ranging from 0 to 10 wt%. These monomer mixtures are initiated by APS and SMBS. For all reactions, EDMA, APS and SMBS concentrations were 0.1, 0.5 and 0.4 wt% of the total monomer, respectively. Polymerization occurred at room temperature and all percentages, unless otherwise stated, are expressed as weight percentages.

2.3. Formulation diagram

A HEMA–MMA–water formulation diagram was created to gain insight into the effect of MMA on the hydrogel microstructure similar to previous formulation phase diagrams for HEMA–ethylene glycol–water [29] and HEMA–EDMA–water [34]. The immiscible boundary in the cast MMA–HEMA–water formulation diagram was determined by adding MMA to a series of HEMA/water mixtures until a monophasic system became immiscible. Immiscibility was defined for a solution that remained biphasic for at least 30 min. The equilibrium water content (EWC) was determined by bulk polymerization of different MMA/HEMA ratios with 1% AIBN at 70°C, followed by swelling in deionized water for 2 weeks, with daily water exchanges.

Table 1
Monomer mixture formulations

Formulation code	Monomer/water (wt% ratio)	HEMA/MMA (wt% ratio)	Formulation of monomer mixture (wt%)		
			HEMA	MMA	H_2O
25-0	25/75	100/0	25.00	0	75
25-1	25/75	99/1	24.75	0.25	75
25-3	25/75	97/3	24.25	0.75	75
25-5	25/75	95/5	23.75	1.25	75
25-7	25/75	93/7	23.25	1.75	75
25-8	25/75	92/8	23.00	2.00	75
25-9	25/75	91/9	22.75	2.25	75
25-10	25/75	90/10	22.50	2.50	75
30-0	30/70	100/0	30.0	0	70
30-1	30/70	99/1	29.7	0.3	70
30-3	30/70	97/3	29.1	0.9	70
30-5	30/70	95/5	28.5	1.5	70
30-7	30/70	93/7	27.9	2.1	70
30-8	30/70	92/8	27.6	2.4	70
30-9	30/70	91/9	27.3	2.7	70
30-10	30/70	90/10	27.0	3.0	70

After dehydrating at 50°C, the EWC was calculated according to the following equation:

$$\mathrm{EWC} = \frac{w_h - w_d}{w_h} \times 100\% \quad (1)$$

where w_h is the hydrated, and w_d the dry mass of the tubes. The boundary between macroporous and microporous pHEMA was determined using scanning electron microscopy of freeze-dried samples.

2.4. Synthesis of p(HEMA-co-MMA) tubes

P(HEMA-co-MMA) tubes were fabricated in custom-built disposable glass molds with an inside diameter (ID) of 2.4 mm, defining the outer diameter of the tube. The relevant quantities of HEMA, MMA, water and APS were added to an amber-colored glass vial, sonicated for 5 min and degassed by purging with helium. The SMBS solution was added and the mixture agitated by swirling for 30 s. The monomer mixture was injected through a 0.45 μm PTFE filter into the polymerization molds, displacing all of the air within the mold. The mold was plugged and placed in the chuck of a horizontally mounted, variable-speed stirring drill with compressed air cooling the glass tube to reduce any heat generated during polymerization. Polymerization proceeded in the rotating molds for a minimum of 5 h at 2500 revolutions per minute (rpm), which was accurately measured with a digital photo tachometer (Model 461893, Extech Instruments, Waltham, MA).

2.5. Phase separation

Phase separation of *cast* formulations using turbidity measurements at 550 nm was conducted with an Ultraspec 4000 spectrometer (Pharmacia Biotech, Canada) as previously described [31,35]. The absorbance of initiated formulations was monitored and the phase separation time determined when a rapid increase in absorbance occurred. Timing began with the addition of SMBS and triplicate time-scans were performed for each formulation.

2.6. Wall morphology

Environmental scanning electron microscopy (ESEM) was used to examine tube wall morphology, allowing the electron imaging of hydrated, uncoated samples [32,33,36]. Cross-sections of hydrated tubes were placed flat on the sample stage of the ESEM (Model E-2020, Electroscan Corporation, USA). Operating conditions include using a vapor pressure of 5–6 Pa, an accelerating voltage of 20 kV, a working distance of 5–7 mm and maintaining the sample temperature at 1 ± 0.2°C with a Peltier-cooled sample stage. Representative images of the wall morphology are reported.

2.7. Surface modification and characterization

The inner surface of the glass mold was silane-modified by applying Sigmacote and air-drying for 30 min. Contact angles of similarly modified and unmodified glass slides were determined in water with a K12 process tensiometer (Krüss, USA) using an

immersion depth of 2 mm for the Wilhelmy plate method ($n = 5$; average ± standard deviation reported).

2.8. Mechanical properties and dimensional analysis

Hydrogel tubes were removed from the glass molds and placed in water for at least 1 day before measurement. The elastic (Young's) modulus of 20 mm length sections was determined in triplicate using a micromechanical tester (Dynatek Dalta) by pulling in tension at a rate of 0.5%/s. The elastic modulus was calculated from the following equation:

$$E = \left(\frac{\sigma}{\varepsilon}\right) = \frac{(\Delta m\, gL)}{(A\, \Delta L)} \tag{2}$$

where g is 9.81 m s^{-2}, L is the length of tube between grips, and $\Delta m/\Delta L$ is the linear slope determined from the micromechanical tester and A is the area of the tube cross-section calculated as shown in Eq. (3). The outside diameter (OD) and ID were measured at two 90° cross-sections per tube with a stereomicroscope (Leica MZ-6) and the area of the cross-section was calculated from the following equation:

$$A = \pi\left[\left(\frac{\mathrm{OD}}{2}\right)^2 - \left(\frac{\mathrm{ID}}{2}\right)^2\right] \tag{3}$$

To create contrast for optical microscopy, the tubes were stained with 0.4% Giemsa methanol stain, then immediately washed in water.

3. Results

Hydrogel tubes were synthesized by liquid–liquid centrifugal casting, as summarized pictorially in Figs. 1a and b. Fig. 2a shows the ternary formulation diagram for *cast* monomer mixtures of MMA–HEMA–water. The respective hydrogels from these monophasic mixtures are either transparent gels, microporous gels, or macroporous cell invasive scaffolds [37]. In the fourth, immiscible region, MMA–HEMA–water hydrogels are heterogeneous due to differences in density. When pHEMA is obtained by polymerization in water in amounts exceeding the EWC, phase separation results in translucent or opaque polymers. The boundary line between transparent and microporous hydrogels is approximated by the EWC of the bulk-polymerized hydrogels, which diminishes with increased amounts of the hydrophobic co-monomer, MMA.

The phase diagram in Fig. 2b demonstrates the importance of phase separation occurring before gelation for the formation of hydrogel tubes by liquid–liquid centrifugal casting, where open circles represent tubes and closed circles represent rods. The boundary line between macroporous and microporous hydrogels approximately separates the monomer systems where phase separation precedes gelation, and vice versa. For those samples well within the microporous region (i.e., 30-0 to 30-3 and 25-0), rods resulted. For those samples within or bordering upon the macroporous region, tubes resulted. The dimensions of all p(HEMA-co-MMA) tubes were constant after being equilibrated in water, indicating that tubes were formed in a swollen state.

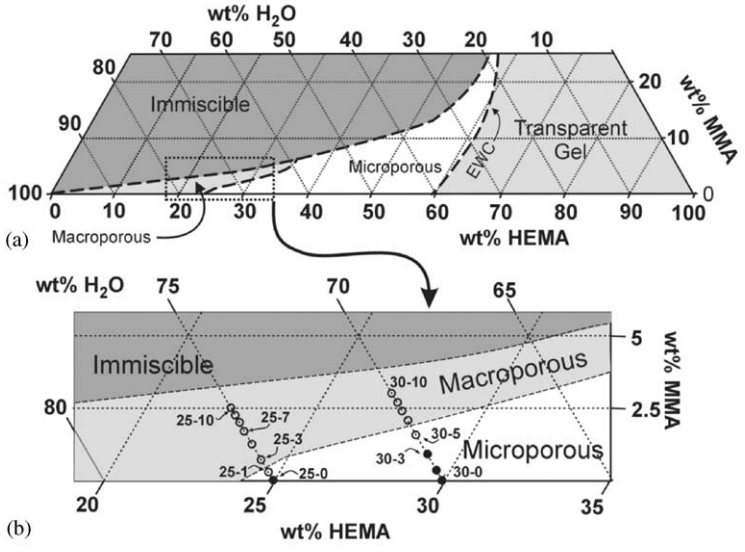

Fig. 2. (a) A formulation diagram of the ternary HEMA–MMA–water system showing the classes of pHEMA–MMA resulting from polymerization at these concentrations and (b) an expanded view of the microporous and macroporous boundary with the hydrogel tube formulations overlaid. Both tubes (○) and rods (●) are formed with codes that are the monomer concentration and MMA percentage of the monomer. The percentages of all components in these formulations are listed in Table 1 under the respective sample codes.

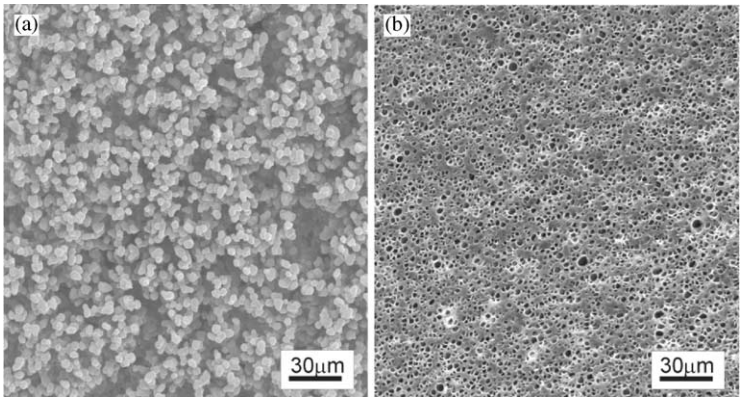

Fig. 3. Electron micrographs of cast (a) macroporous and (b) microporous pHEMA.

For macroporous structures to form, the monomer phase must separate prior to gelation to form a structure that is cell-invasive (Fig. 3a). When gelation precedes phase separation, microporous pHEMA gels form that have few (if any) interconnecting pores and are not cell-invasive (Fig. 3b). The resulting morphology is considerably different between microporous and macroporous pHEMA hydrogels as shown in Fig. 3. Similar SEM images were decisive in determining the boundary between microporous and macroporous hydrogels.

MMA accelerates the onset of phase separation in HEMA/water formulations. As shown in Fig. 4, as MMA concentration increases from 0% to 10%, the time to phase separate decreases, from ~400 to 105 s for the formulation with 30% monomer and from 310 to 140 s for a formulation with 25% monomer. Microporous formulations (i.e. 25-0, 30-0 and 30-3 compositions) gel before phase separating and thus require longer times for phase separation than macroporous formulations, which phase separate first.

Fig. 5 shows micrographs of tubes prepared with formulations containing 25% monomer, of which the MMA concentration ranged from 5% to 10%, the remainder of which is HEMA. As shown in Fig. 5a, a tube prepared from 5% MMA has a two-layered wall morphology that appears to have some radial orientation when observed with a stereomicroscope. ESEM imaging of the wall shows that the outer layer is a gel with closed cell pores and the inner layer is comprised of phase-separated particles, or polymer droplets. For 7% MMA (Fig. 5b), the tube wall is predominantly gel-like with very few pores and a relatively thin inner porous layer. Tubes made with 10% MMA have less gel, and consist predominantly of phase-separated particles (Fig. 5c). There also appears to be some radial orientation within the porous component of the tube wall, though this has not been quantified. The polymer particles in the inner phase of the tube appear to decrease in size approaching the lumen.

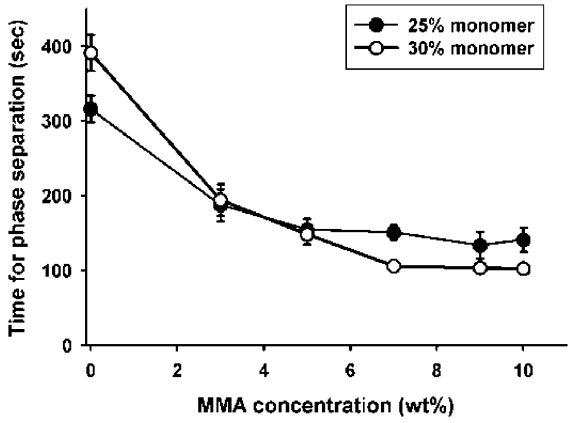

Fig. 4. Graph of phase separation time with respect to MMA concentration of cast formulations. Phase separation was determined by absorbance at 550 nm in triplicate (mean ± standard deviations are plotted).

Fig. 6 shows the morphology of a tube made with 30% monomer, 10% of which is MMA. Fig. 6a shows the concentric tube in cross-section by light microscopy, which is more easily observed expanded in Fig. 6b by SEM, where radial cracks can be seen but are only continuous through the wall at some points. The outer surface of the tube shows a spotted or cracked appearance that is best depicted in Fig. 6c. When the inside surface of the glass mold is silane-modified to be hydrophobic, the outer morphology is plain and the wall morphology of the 30% monomer formulation (Fig. 6d) resembles that of the 25% monomer formulation (Fig. 5b). The dynamic advancing and receding water contact angles of unmodified and modified glass slides were found to be $45\pm3/12\pm2^{\circ}$ and $47\pm1/44\pm1^{\circ}$, respectively.

As shown in Fig. 7, the elastic (or Young's) modulus of the tubes increased with MMA concentration, reflecting the importance of the gel phase to the overall mechanical properties of the tube. The increased

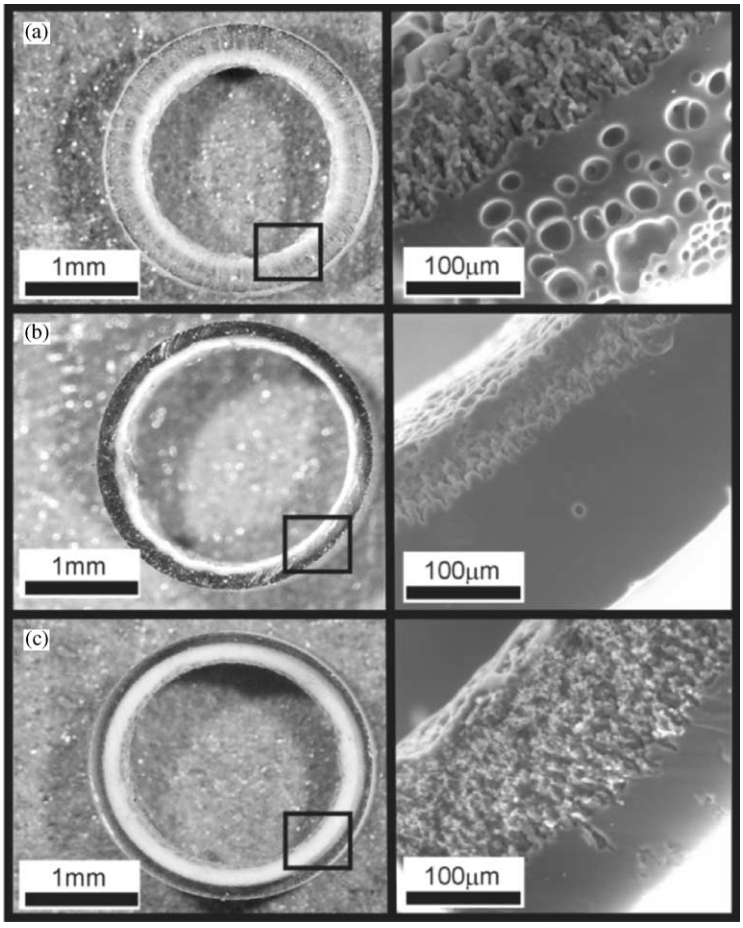

Fig. 5. Representative optical and ESEM micrographs of tubes made with 25% monomer of which (a) 5% is MMA, (b) 7% is MMA and (c) 10% is MMA.

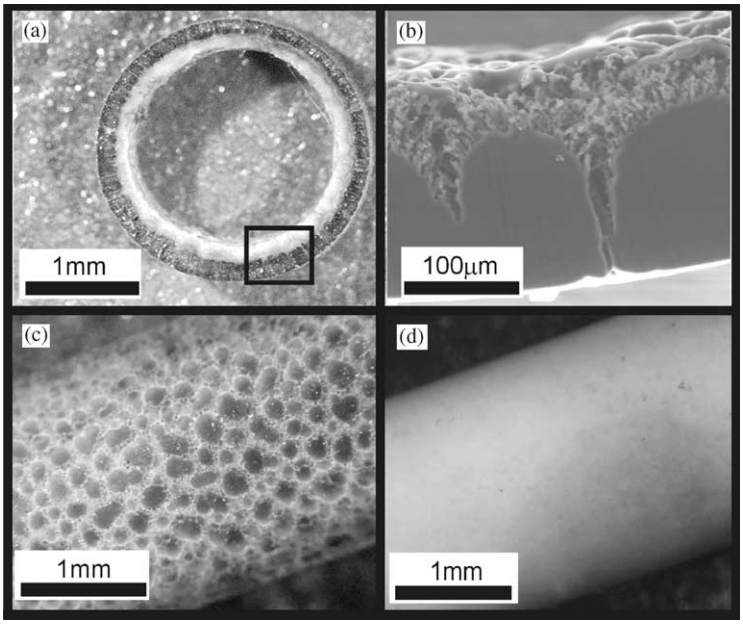

Fig. 6. Representative optical and ESEM micrographs of tubes made with 30% HEMA, 10% of which is MMA cut (a) in cross-section and (b) in cross-section using ESEM and (c) in longitudinal view. A tube synthesized with the same formulation as in (c), but spun in a silane-treated glass mold is shown in (d).

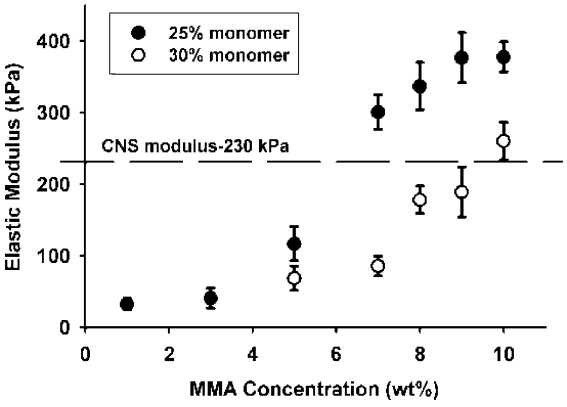

Fig. 7. Graph of the hydrogel tubes elastic modulus with respect to MMA concentration. The target modulus of 230 kPa for spinal cord tissue is superimposed.

modulus also reflects the reduced swelling of the hydrogel with higher concentrations of the hydrophobic MMA co-monomer incorporated within the polymer chain. Interestingly, the average elastic modulus of tubes made with 30% monomer is lower than that of 25% tubes, likely because of the discontinuous gel phase, as was shown in Figs. 6b and c.

4. Discussion

As we previously demonstrated with homopolymeric pHEMA tubes, phase separation must occur prior to gelation for p(HEMA-co-MMA) tubes to form [26]. This is demonstrated in Fig. 2b, where microporous formulations close to the boundary resulted in rods, whereas tubes were predominantly formed when a macroporous formulation was used. If the polymerizing mixture forms a gel before phase separation, the hydrogel fills the entire mold, resulting in a rod. This phenomenon was observed for tubes having 30% monomer with low MMA ($\leqslant 3\%$); these correspond to a formulation for microporous gels, where gelation precedes phase separation (Fig. 2b). Increasing the MMA concentration affects the solubility of the propagating radical in the monomer mixture and promotes phase separation over gelation. Indeed, phase separation times were shown to decrease with increasing MMA concentration (Fig. 4). With fast phase separation times, the separated phase displays liquid-like behavior, consisting of monomer enriched with short propagating radical chains and water equivalent to EWC; this liquid character is required for coalescence of the separated droplets into the gel phase.

The distinct wall morphology of p(HEMA-co-MMA) tubes, with a gel-like outer layer and a porous inner layer, reflects the changes in viscoelastic properties of the phase-separated particles throughout polymerization. The first particles to be phase separated are predominantly liquid-like, and coalesce together to form the continuous gel phase on the outer part of the wall. Particles that phase separate towards the latter stages of polymerization do not coalesce, likely due to the increased elastic nature of the particles. This results in a porous, or spongy, inner layer that is seen with all hydrogel tubes manufactured in this process. As was implied by Fig. 5c for 25% monomer tubes, the particle droplet size within the wall appears to decrease towards the lumen. This may result from solubility changes during conversion, as HEMA serves both as a co-monomer during polymerization and a solvent for the propagating radical. Previous studies have shown that phase-separated pHEMA droplets diminish in size with increased water concentration in the monomer mixture [29]. Near full conversion, when the majority of the polymer has phase separated, the center of the mold is enriched with water and thus the separating phase likely becomes insoluble as smaller droplets. For 25% monomer tubes, a maximum relative thickness of the gel phase in the wall structure is reached at 7% MMA content. This also correlates with the middle of the macroporous region in the formulation diagram, between the microporous and immiscible regions (Fig. 2b). This suggests that there may be an optimum solubility for the monomers and solvent within the macroporous region, resulting in tubes that are almost fully gel-like, compared to those of either 5% or 10% MMA content tubes.

Fig. 7 demonstrates that both 25% and 30% monomer tubes with MMA concentrations approaching 10% have an elastic modulus approaching the target value of 230 kPa. However, as we previously demonstrated, the wall morphology and transport properties of similar pHEMA–MMA tubes formed by liquid–liquid centrifugal casting are vastly different [38], with diffusive permeability varying between 10^{-7} and 10^{-9} cm^2/s. The rigidity of the tubes increases with MMA concentration, as would be expected from incorporating a hydrophobic monomer into a hydrophilic polymer network. While one might have expected the higher monomer concentration to result in a stronger tube, this was not true due to the morphology seen in the 30% monomer formulations. As was shown in Fig. 6c, the outer surface of the tube is cracked and cross-sections reveal a highly porous wall morphology. The liquid-like phase-separated monomer appears to bead on the inner surface of the glass mold where its structure is fixed by gelation. With high MMA concentrations, the separated polymer-swollen monomer is relatively hydrophobic and liquid-like, allowing it to form a droplet on the hydrophilic glass mold surface. We tested this beading hypothesis by coating the inner surface of the glass mold with a silane-coupling agent (Sigmacote), thereby changing the wettability of the glass mold from hydrophilic to

hydrophobic. On hydrophobic surfaces, monomer beading is reduced and spreading permitted, thereby producing a smooth outer surface and a wall morphology (Fig. 6d) that resembles that of the 25% monomer formulation (Fig. 5b). Varying the surface chemistry of the mold can therefore affect the wall morphology, and mechanical properties as shown herein.

5. Conclusions

Liquid–liquid centrifugal casting of poly(HEMA-co-MMA) results in tubes with diverse morphologies, wall thicknesses and mechanical properties that are similar to that of the spinal cord. The manufacturing process involves a balance of centrifugal forces, solubility, polymer kinetics and density differences. By controlling the formulation chemistry and surface chemistry of the mold, hydrogel tubes result with a range of wall morphologies and mechanical properties.

We envision using these tubes as a component of a tissue-engineered device for spinal cord injury repair. The elastic modulus of the spinal cord can be approximated with p(HEMA-co-MMA) nerve guides and their biocompatibility in the central and peripheral nervous systems is currently being assessed. Preliminary results indicate the promise of these hydrogel tubes in such applications [32,33].

Acknowledgements

The authors thank Shaily Sanghvi for technical assistance and thank Klaus Schultz (Botany, McMaster University) for use of the ESEM. The technical assistance of Dan Lousenberg during processing development is also appreciated. The authors gratefully acknowledge support from The Whitaker Foundation Biomedical Engineering Research Grant and the Natural Sciences and Engineering Research Council of Canada.

References

[1] Chirila TV. An overview of the development of artificial cornea with porous skirts and the use of PHEMA for such an application. Biomaterials 2001;22(SI):3311–7.
[2] Park H, Park K. Hydrogels in bioapplications. ACS Symp Ser 1996;627:2–10.
[3] Peppas NA, Huang Y, Torres-Lugo M, Ward JH, Zhang J. Physicochemical foundations and structural design of hydrogels in medicine and biology. Annu Rev Biomed Eng 2000;2:9–29.
[4] Kennedy JP, Fenyvesi G, Na S, Keszler B, Rosenthal KS. Synthesis and characterization of tubular amphiphilic networks with controlled pore dimensions for insulin delivery. Des Mon Pol 2000;3:113–22.
[5] Li RH, Altreuter DH, Gentile FT. Transport characterization of hydrogel matrices for cell encapsulation. Biotechnol Bioeng 1996;50:365–73.
[6] Den Dunnen WFA, Van Der Lei B, Schakenraad JM, Stokroos I, Blaauw E, Bartels H, Pennings AJ, Robinson PH. Poly(DL-lactide-ε-caprolactone) nerve guides perform better than autologous nerve grafts. Microsurgery 1997;17:348–57.
[7] Chamberlain LJ, Yannas IV, Hsu HP, Strichartz G, Spector M. Collagen-GAG substrate enhances the quality of nerve regeneration through collagen tubes up to level of autograft. Exp Neurol 1998;154:315–29.
[8] Tunturi AR. Elasticity of the spinal cord dura in the dog. J Neurosurg 1977;47:391–6.
[9] Hung TK, Chang GL, Lin HS, Walter FR, Bunegin L. Stress–strain relationship of the spinal cord of anesthetized cats. J Biomech 1980;14:269–76.
[10] Tunturi AR. Elasticity of the spinal cord, pia, and denticulate ligament in the dog. J Neurosurg 1978;48:975–9.
[11] Chang GL, Hung TK, Feng WW. An in-vivo measurement and analysis of viscoelastic properties of the spinal cord of cats. J Biomech Eng 1988;110:115–22.
[12] Ramon-Cuerto A, Plant GW, Avila J, Bunge MB. Long distance axonal regeneration in the transected adult rat spinal cord is promoted by olfactory ensheathing glia transplants. J Neurosci 1998;18:3803–15.
[13] Menei P, Montero-Menei C, Whittemore SR, Bunge RP, Bunge MB. Schwann cells genetically modified to secrete BDNF promote enhanced axonal regrowth across transected adult rat spinal cord. Eur J Neurosci 1998;10:607–21.
[14] Bamber NI, Li H, Lu X, Oudega M, Aebischer P, Xu XM. Neutrophins BDNF and NT-3 promote axonal re-entry into the distal host spinal cord through Schwann cell-seeded mini-channels. Eur J Neurosci 2001;13:257–68.
[15] Xu XM, Guenard V, Kleitman N, Bunge MB. Axonal regeneration into Schwann cell-seeded guidance channels grafted into transected adult rat spinal cord. J Comp Neurol 1995;351:145–60.
[16] Plant GW, Harvey AR. A new type of biocompatible bridging structure supports axon regrowth after implantation into the lesioned rat optic tract. Cell Transplant 2000;9:759–72.
[17] Bloch J, Fine EG, Bouche N, Zurn AD, Aebischer P. Nerve growth factor and neurotrophin-3-releasing guidance channels promote regeneration in the transected rat dorsal root. Exp Neurol 2001;172:425–32.
[18] Liu S, Bodjarian N, Langlois O, Bonnard AS, Boisset N, Peulvé P, Saïd G, Tadié M. Axonal regrowth through a collagen guidance channel bridging spinal cord to the avulsed C6 root: functional recovery in primates with brachial plexus injury. J Neurosci Res 1998;51:723–34.
[19] Chamberlain LJ, Yannas IV, Hsu HP, Strichartz G, Spector M. Collagen-GAG substrate enhances the quality of nerve regeneration through collagen tubes up to level of autograft. Exp Neurol 1998;154:315–29.
[20] Greenwald SE, Berry CL. Improving vascular grafts: the importance of mechanical and haemodynamic properties. J Pathol 2000;190:292–9.
[21] Salacinski HJ, Goldner S, Giudiceandrea A, Hamilton G, Seifalian AM, Edwards A, Carson RJ. The mechanical behavior of vascular grafts: a review. J Biomater Appl 2001;15:241–78.
[22] Moore WR, Graves SE, Bain GI. Synthetic bone graft substitutes. ANZ J Surg 2001;71:354–61.
[23] Woerly S, Pinet E, De Robertis L, Bousmina M, Laroche G, Roitback T, Vargova L, Sykova E. Heterogeneous PHPMA hydrogels for tissue repair and axonal regeneration in the injured spinal cord. In: Polymers for tissue engineering. Utrecht, Netherlands: VSP, 1998. p. 343–73.
[24] Mokry J, Karbanova J, Lukas J, Paleckova V, Dvorankova B. Biocompatibility of HEMA copolymers designed for treatment of

CNS diseases with polymer-encapsulated cells. Biotech Prog 2000;16:897–904.
[25] Plant GW, Chirila TV, Harvey AR. Implantation of collagen IV/poly(2-hydroxyethyl methacrylate) hydrogels containing Schwann cells into the lesioned optic tract. Cell Transplant 1998;7:381–91.
[26] Dalton PD, Shoichet MS. Creating porous tubes by centrifugal forces for soft tissue applications. Biomaterials 2001;22:2661–9.
[27] Yasuda H, Gochin M, Stone W. Hydrogels of poly(hydroxyethyl methacrylate-glycerol monomethacrylate copolymers. J Polym Sci A 1;4:2913–27.
[28] Dalton PD, Vijayasekaran S, Shoichet MS. Processing of polymer scaffolds: polymerization. In: Methods of tissue engineering. San Diego, CA: Academic Press, 2001. p. 725–31.
[29] Chirila TV, Chen YC, Griffin BJ, Constable IJ. Hydrophilic sponges based on 2-hydroxyethyl methacrylate. 1. Effect of monomer mixture on the pore size. Polym Int 1993;32:221–32.
[30] Clayton AB, Chirila TV, Dalton PD. Hydrophilic sponges based on 2-hydroxyethyl methacrylate. III. Effect of incorporating a hydrophilic crosslinking agent on the equilibrium water content and pore structure. Polym Int 1997;42:45–56.
[31] Lou X, Dalton PD, Chirila TV. Hydrophilic sponges based on 2-hydroxyethyl methacrylate. VII. Modification of sponge characteristics by changes in reactivity and hydrophilicity of cross-linking agents. J Mater Sci Mater Med 2000;11:319–25.
[32] Dalton PD, Tsai E, Van Bendegem RL, Tator CH, Shoichet MS. Hydrogel nerve guides promote regeneration in the central nervous system. Tampa Bay, FL: Society for Biomaterials, 2002.
[33] Midha R, Munro CA, Dalton PD, Tator CH, Shoichet MS. Novel biocompatatible tube enhanced with growth factors support peripheral nerve regeneration. Cancun, Mexico, American Society for Peripheral Nerve 2002.
[34] Šprincl L, Kopecek J, Lim D. Effect of structure of poly(glycol monomethacrylate) gel on calcification of implants. Calcif Tissue Res 1973;13:63–72.
[35] Chirila TV, Higgins B, Dalton PD. The effect of synthesis conditions on the properties of poly(2-hydroxyethyl methacrylate) sponges. Cell Polym 1998;17:141–62.
[36] Danilatos GD. Introduction to the ESEM instrument. Microsc Res Tech 1993;25:354–61.
[37] Chirila TV, Constable IJ, Crawford GJ, Vijayasekaran S, Thompson DE, Chen YC, Fletcher W, Griffin BJ. Poly(2-hydroxyethyl methacrylate) sponges as implant materials: in vivo and in vitro evaluation of cellular invasion. Biomaterials 1993;14:26–38.
[38] Luo Y, Dalton PD, Shoichet MS. Novel poly(HEMA-MMA) hydrogel hollow fiber membranes: morphology and properties. Chem Mater 2001;13:4087–93.